STATIC LIQUID INTERFACE TO REDUCE SUPPORT STRUCTURE NECESSITY IN TOP-DOWN STEREOLITHOGRAPHY

Nicholas Mulka, Tarun Goyal, Amit Jariwala, David Rosen

Georgia Institute of Technology, Atlanta, GA 30332

Abstract:

Stereolithography (SLA) 3D printing is a vat photopolymerization additive manufacturing process that utilizes photocurable resin, which requires sacrificial supporting structures on part overhangs, increasing material waste and post-processing time. This study details a novel process for conducting top-down SLA 3D printing from a thin resin layer located above a static immiscible supporting fluid, which reduces or eliminates the need for solid supports. The support fluid prevents deflection from buoyant and gravitational forces on thin overhangs from anchored parts due to minute density differences between the supporting fluid and cured resin, while reducing the volume of resin necessary to print compared to traditional top-down SLA. Using this process, we have experimentally demonstrated printed geometry with overhangs of up to 90 degrees. Additionally, necessary material properties of both fluids and process parameters of the system have been identified for the system's feasibility and broader adaptation.

Introduction:

Additive manufacturing (AM) for the purpose of rapid prototyping is a well developed technology, however its adoption has the potential to become more widespread, particularly for the use of industrial manufacturing [1]. Stereolithography (SLA) 3D printing has been popularized because of the detailed and complex structures it can create. SLA 3D printing utilizes resin containing UV-sensitive photoinitiators that enable a cross linking process, turning liquid monomers into solid polymers when exposed to UV light. With precise shining of UV light onto a layer of resin, a solid three dimensional object can be created, either layer-by-layer or continuously [2]. One drawback of this printing process is the need for solid, sacrificial support structures below overhanging geometry to counteract the forces of gravity. Printing these structures increases the print time and wastes valuable photosensitive resin. The process of removing these structures requires expensive manual labor, adds manufacturing time, and leaves a rough surface finish. As a result, research has been conducted in eliminating sacrificial supports or mitigating their drawbacks in SLA printing and AM in general.

Concepts for mitigating the challenges of support structures have been developed for other methods of additive manufacturing. For example, the use of soluble support structures in fused deposition modeling (FDM) is already a commercially available technology [3]. This method would not be possible in most commercial SLA printers as they are only able to print with a single liquid resin. Yigit and Lazoglu propose a dynamic print bed which can change

shape to support overhangs as a part is printed with powder-based AM [4]. Several studies have been conducted on optimizing support structures to minimize their necessity and size in SLA printing specifically [5, 6, 7]. However, these studies do not suggest a method of printing that minimizes the need for parts to be supported. Lee et al. demonstrate an SLA 3D printer which produced a micro-scale structure without support structures [8]. This printing system, however, does not indicate support structure reduction when scaled to larger geometries.

This study proposes a novel Fluid Interface Supported Printing (FISP) process for conducting top-down SLA 3D printing which reduces the need for sacrificial support structures below overhanging geometry. Bhanvadia et al. use a static liquid constrained interface utilizing Fluorinert, to conduct both continuous and layer-by-layer SLA printing. This system is capable of printing overhangs of approximately 1.5mm without sacrificial supports [9]. Using a bottom-up curing approach, they have recently demonstrated the feasibility of printing high resolution prints with the liquid interface. The associated patent application for "three-dimensional fabrication at inert immiscible liquid interface" [10] contains the details of their fluid interface printing system. Another relevant patent is from Carbon for their "continuous three dimensional fabrication from immiscible liquids" [11]. The proposed systems detailed in the patents and the FISP process share many similarities; utilizing an inert immiscible liquid in conjunction with a photopolymerizable liquid to fabricate three dimensional objects. The FISP process is novel via the process of retaining the cured geometry inside of the inert liquid throughout the printing process instead of air or the photopolymerizable liquid and due to both patents detailing photopolymerization occurring after the irradiating UV light passes through some portion of the inert immiscible liquid. Retaining the polymerized resin in the inert liquid, or supporting fluid, after curing enables the mitigation of buoyancy and gravitational forces propagating from differences in density between the polymerized resin and the medium in which it is resting within. This gap in existing literature prompts further investigation into the applications of liquid interface supported production for stereolithography.

SLA printing continues to be the target for improvement because of the opportunity for isotropic parts and detailed features. A method which minimizes post-processing time and expense by largely eliminating the need for support structures would be a valuable addition to SLA technology. This change will also allow for smoother surface finishes, compounding an existing advantage of SLA printing. However, this process must be scalable to accommodate large objects while minimizing the material and operation cost. Additional features might include the ability to manufacture parts for certain applications like fluidic devices or clear parts for optical use. The effectiveness of using a type of fluid interface with resin printing has been demonstrated previously, and provides an opportunity for continued improvement and implementation.

Methods:

In order to implement a fluid-interface based printing process, a top-down SLA setup was designed and utilized for experimentation. Like commercially available SLA printers, this setup uses UV light to cure photosensitive resin in successive thin resin layers and build up a 3D structure. This system consists of a movable optical setup positioned above a three-phase interface consisting of a fluorinated ethylene propylene (FEP) film, a thin layer of photosensitive resin, and a supporting fluid. Within this interface a build platform is positioned, and is used to locate the part. The build platform is not necessarily flat and can be changed to accommodate different testing scenarios. Figure 1 displays a diagram of the printing setup and a labelled picture.
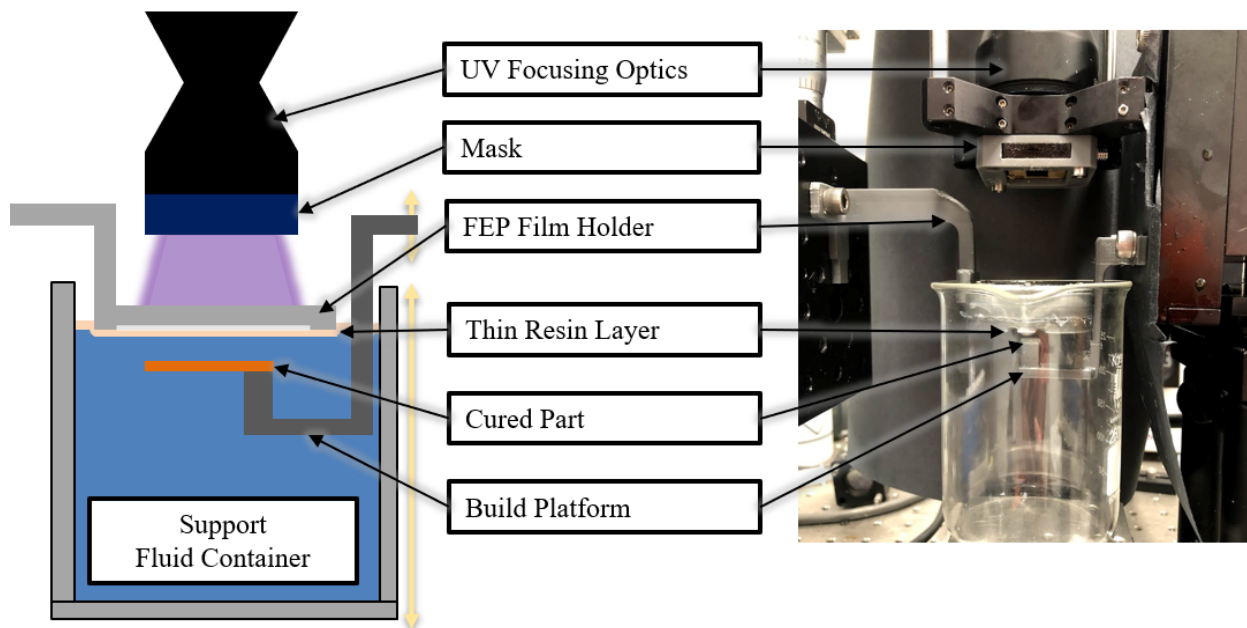

Figure 1: Setup of the fluid interface support printing system

The optical setup consists of a UV light source, a system of lenses, and an opaque light mask. This assists in refining UV light that is then projected through a mask, onto the FEP film, and into the photosensitive resin, which then hardens to create a layer of the 3D part. Specific cross-sections are defined by removable masks that are fixed on a mount between the light source and print area. One of the lenses is a Galilean beam expander (Thorlabs GBE03-A), which helps partially collimate the light, resulting in a beam angle of 8.5 degrees. This imperfect collimation results in changes in the part dimensions depending on where the printing interface is relative to the light. The light homogeneity has not been quantified, but has been observed to be negligible at the current operating scale. It is possible to adjust the intensity of the light by adjusting the distance of the lens from the FEP film or by adjusting the collimation knob on the beam expander. This optical setup is able to move parallel to the print area using a motorized platform.

The FEP film is tensioned using a custom mount and gives a printing area of 35.75 x 26.00 mm^2. The film is lowered until it is in contact with the top surface of the photosensitive resin which rests in a thin layer above the supporting fluid. The resin is supported by the fluid beneath it, and the printed part is anchored at its base by a mobile build platform. The build platform moves downward through the support fluid as the print proceeds to allow another layer of the part to be printed. The FEP film provides a surface which the printed part can adhere to during curing. The adhesion to the film reduces deflection caused by internal stresses of crosslinking while the part cures. Because the FEP film is oxygen permeable, an oxygen deadzone is created close to its surface which prevents the resin from curing to the FEP film and permanently adhering [12]. Though the FEP film inhibits parts printing to its surface via oxygen inhibition, printed parts experienced stiction [13], where the two very smooth surfaces of the FEP and solidified cantilever beam adhere together and need to be pulled apart. Adhering to the FEP film is not permanent, as oxygen inhibition prevents bonding between the cured resin and the film, preventing damage to the printed part.

The resin used in SLA printing contains at least a base monomer which is ready to be polymerized, and a photoinitiator which, when exposed to UV light, begins a crosslinking process to solidify and harden the resin. In traditional top-down SLA, a vat of resin is filled according to the height of the desired object. Taller objects must have a taller vat filled with more resin, even if the volume of the part would not require all the resin used. In the proposed system, the support fluid would replace the vast majority of the resin in the vat, allowing for the volume of resin deposition in top-down printing to match the expected print volumetric requirements. Bottom-up style SLA printers get around the requirement of filling a vat full of resin by using a thin layer of resin at the bottom of the printer. Parts printed in bottom-up printers, however, do not have surrounding resin providing upwards buoyancy to parts like in top-down printers, exposing parts to gravitational forces. This drives the primary motivation behind investigation of the Fluid Interface Supported Printing (FISP) process. The FISP process aims to achieve a neutrally buoyant printed part in the support solution. A simple consideration of forces on the printed part will be offered, where specific forces are identified symbolically as (F_x). When a layer is finished curing and is being removed from the FEP film, it experiences adhesion and stiction forces from the FEP (F_{ad}), surface tension between the cured parts and the resin fluid interface (F_γ), buoyant force from the support fluid (F_B), and gravity (F_g). Matching the density of the supporting fluid to that of the resin enables the cured part to be neutrally buoyant, and allows for the uncured resin to rest on top of the support fluid. The forces associated with the removal of a cured layer from the FEP film are outlined in Figure 2.
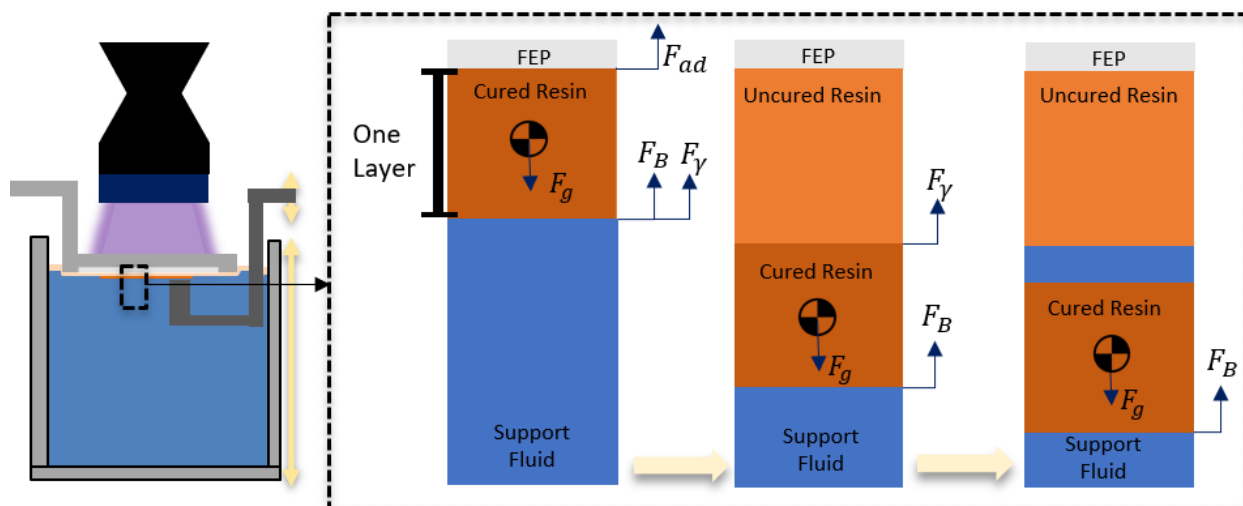
Figure 2: Forces associated with removing a cured layer from the FEP film.

A matching density of supporting fluid and cured resin theoretically enables large structures to be printed with no net force inside of the supporting fluid. This assumes, however, that the print can withstand the forces associated with removal from the FEP film and the interfacial surface tension. The resin and supporting fluid must be immiscible to maintain the interface surface, prevent resin contamination, and minimize material degradation. Low viscosity in the supporting fluid is desired to minimize the forces which act on structures when prints are moved down during printing, and increase surface spreading of resins. A water based solution was chosen for the supporting fluid, and sodium-chloride was added to adjust fluid density to support the liquid resin layer while resembling the density of the cured resin layers. A 20%wt solution of sodium-chloride was created to increase the density of the supporting fluid to 1.145 g/mL. The polarity of water assists in maintaining immiscibility between itself and a nonpolar resin. Thus, the resin must have a density of less than 1.145 g/mL, must be immiscible in water, and have minimal viscosity. 1,6-Hexanediol diacrylate (HDDA) was chosen as a candidate resin for its immiscibility with water (< 0.1 mg/mL), density (1.02 g/mL), viscosity (9 cP) [14], and its availability. While HDDA was chosen as the primary resin monomer, an additive was desired to increase the surface spreading of the resin. Low viscosity in the resin is desired to assist in refilling the uncured resin film across the FEP film between layers. Figure A1 details differences in the important properties for various resin additives that were considered. 2-Ethylhexyl acrylate (EHA) and was chosen as the primary candidate for resin spreading testing due to its low density (0.885 g/mL), reduced viscosity (1.7 cP), and immiscibility with water (< 0.1 mg/mL). Testing was conducted to determine the optimal amount of EHA additive based on its spreading over the saline supporting fluid. In this testing, different resin compositions were deposited on a saline supporting fluid and the contact area of the droplet was measured over time. The speed of this droplet expansion was used to determine the spreadability of the resin composition. The area of the droplet was calculated using vector graphics software and a reference object of known size

placed at the water level. Figure 3 provides data which shows the resin composition against its spreading characteristics, alongside images of selected experiments.

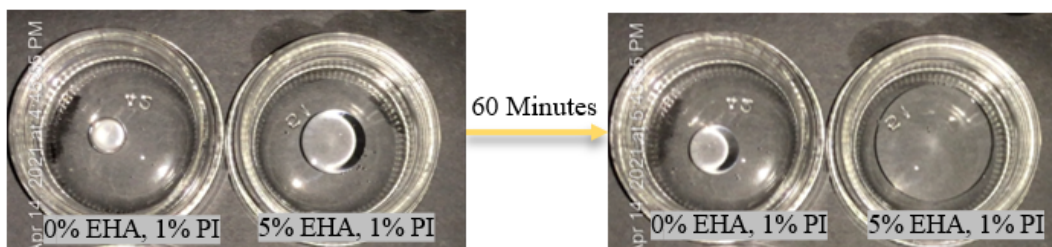| Composition (molar %)	Initial Area (t = 0m)	Final Area (t = 60m)	% Change
0% EHA, 1% PI, 99% HDDA	1.02 cm^2	1.76 cm^2	72.50%
1% EHA, 1% PI, 98% HDDA	1.87 cm^2	6.77 cm^2	262.80%
5% EHA, 1% PI, 94% HDDA	2.12 cm^2	7.77 cm^2	266.40%
10% EHA, 1% PI, 89% HDDA	2.91 cm^2	10.1 cm^2	248.00%

Figure 3: Spreading comparison for different molar percentages of EHA.

A 5% molar EHA solution was shown to exhibit the greatest relative change in spreading of the tested options. The photoinitiator (PI) used in the system was chosen to be 2,2-Dimethoxy-2-phenylacetophenone (DMPA) due to its availability and documented crosslinking compatibility with HDDA [15]. The amount of photoinitiator was varied and optimized experimentally to determine feasible operating ranges of the FISP system.

Results and Discussion:

To determine what parameters resulted in successful unsupported printed parts, experiments of cantilever beam prints were conducted by varying the process parameters of light intensity, time of exposure, and the molar percentage of the photoinitiator in the resin. The cantilever geometry was chosen because it is the most extreme example of a structure that requires solid supports, which arises from the cantilever's 90 degree overhang and resulting internal moment. Successful cantilever prints are defined as photopolymerized beams that do not break off of the FEP film when removed, display minimal curling upwards or downwards after removal, and display similar geometric shape outlined by the mask. The dimensions of the print results were based on the location of the tests relative to the 20mm x 10mm mask, due to the UV-light not being perfectly collimated with a 8.5 degree beam angle. Print tests were performed for photoinitiator compositions of 2.5%, 5%, 10%, 15%, and 20% PI molar concentration. All tests were performed with 5% molar EHA composition to assist with surface spreading and to reduce the viscosity of the resin. Incident UV intensity was varied between 10mW, 13.75mW, and 15.5mW, and the time of exposure was varied between 3 and 12 seconds. All intensity measurements are conducted at a wavelength of 365nm and over an area of 7.088e-05mm^2. Up to 2mL of resin was deposited on the surface of the supporting fluid for each experimental trial.

When curing a thin, unsupported cantilever beam, the degree of conversion inside the resin layer becomes an important factor when determining the behavior of the beam. When the molar photoinitiator percentage is low, the degree of oxygen inhibition relative to the free radical concentration is high, causing the deadzone thickness to increase [16]. Conversely, high photoinitiator concentrations and incident irradiance causes the deadzone to disappear [15], and the resin cures to the surface of the FEP film. Figure 4 details the curing behavior of a single layer in the FISP system.
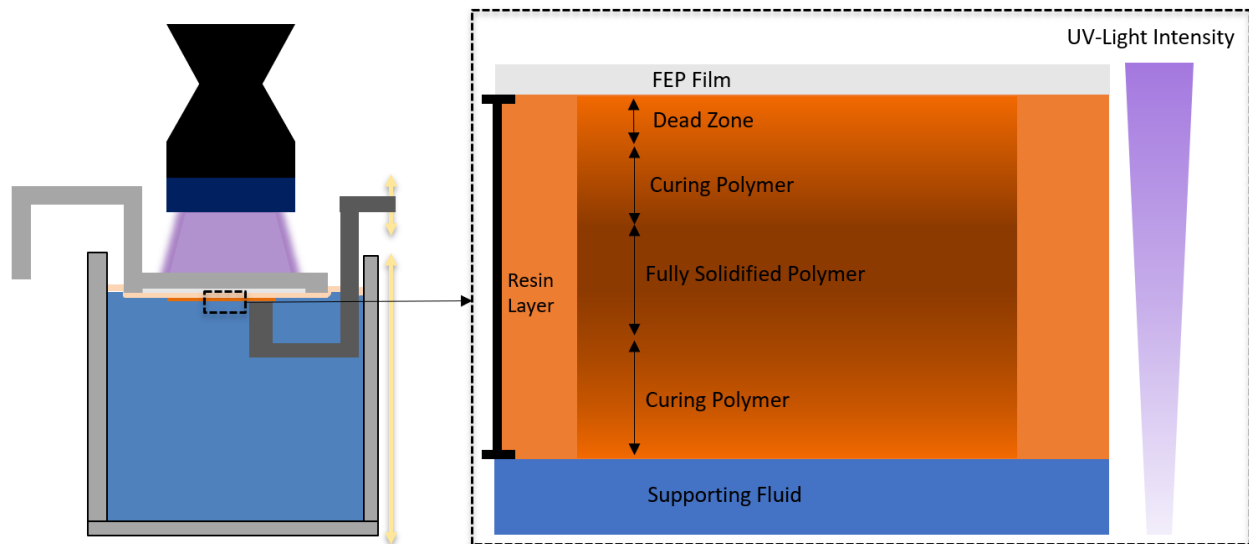

Figure 4: Non-uniform cross linking behavior within the resin layer due to UV-light absorbance and oxygen inhibition during curing.

Balancing the depth of penetration of the UV-light and the free-radical oxygen inhibition is necessary to minimize solidified part warping. Resin formulations for 2.5% and 5% molar concentrations of DMPA yielded cantilever beam prints which repeatedly delaminated from the FEP film for a large range of the intensities and times tested. From analysis of video footage, delamination from the film could be rapid, with overhangs warping up to a vertical distance of 7.5mm in 0.12 seconds in the support solution. Internal stresses in the cure cause this deflection, theorized to be due to a large degree of oxygen inhibition causing the highest degrees of crosslinking to happen near the bottom of the layer, shrinking it relative to the rest of the cantilever beam print. When the photoinitiator concentration was increased to 10% molar PI, a significant reduction in delamination from the FEP film between subsequent layers was observed. Resulting cure behavior is outlined for several print times for 10% molar PI in Figure 5.
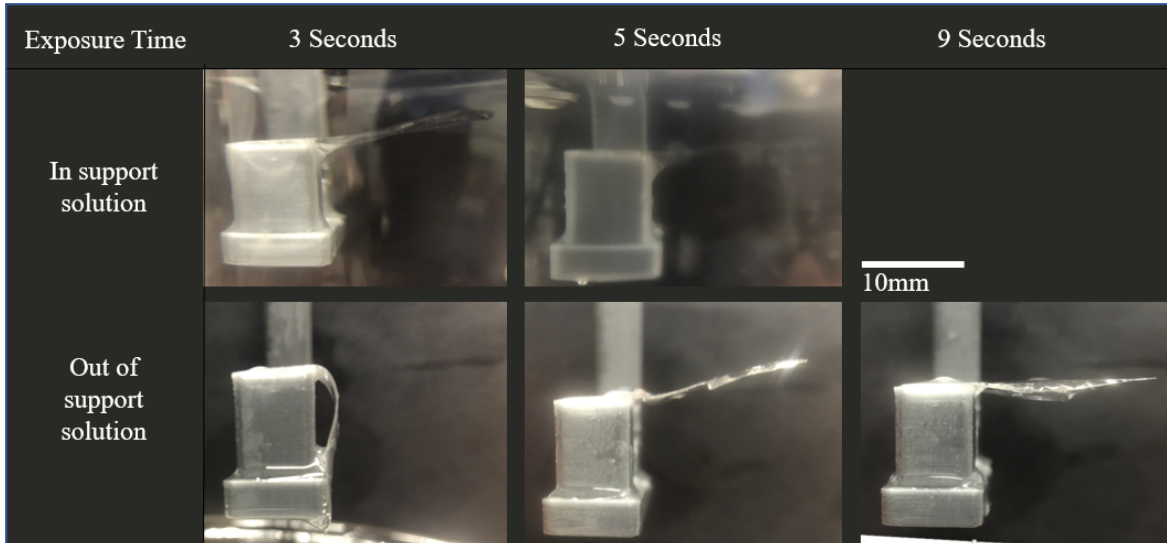
Figure 5: Comparison of different exposure times for a 10% molar DMPA, 5% molar EHA solution exposed to 15.5mW of UV light, inside and outside of the supporting solution.

For low energy doses, i.e. 3 seconds at 15.5mW, the resulting cantilever beam would have a low degree of crosslinking conversion. This makes it susceptible to bending downwards due to gravity once removed from the supporting solution. Cantilever deflection inside of the supporting solution comes primarily from internal stresses in the print, as the density differences between the supporting solution and the cured part will not cause substantial deflection. The three second exposure test is a good candidate to revisit for multi-layer prints in the future to assess the neutral buoyancy of the FISP system. For this PI concentration and UV intensity, beams that were made at 5 seconds of exposure consistently display sufficient crosslinking to support their own weight, but residual cross linking and shrinkage strains [17] after the UV-exposure cause the beam to curl upwards. The upward curl from residual stresses in the beam may not be present immediately after the print is removed; as the pictures from the five second exposure time experiment do not display the warping behavior until some time after the removal of the print from the FEP film. This is known as a dark reaction [18]. When the time of exposure is increased for this resin combination, many of the residual free radicals present in the system more fully crosslink the monomer, reducing the dark reaction and solidifying the part. The beam's higher degree of crosslinking produces cantilever beams that are a single, self-supporting layer. The increased crosslinking of the resin combination leads to stiffer parts that are able to overcome F_{ad} and F_{γ} when being removed from the FEP film. Increasing the photoinitiator concentration increases the rate of crosslinking in the curing layer [19]. Increasing the molar photoinitiator composition to 20% in the resin layer increases the rate of crosslinking throughout the resin while creating a uniform and sturdy beam. However, due to the relatively large amount of photoinitiator present in the resin, the oxygen inhibition from the permeable FEP film cannot overcome the number of free radicals present under the irradiance of the UV-light, and the parts tend to cure to the FEP film. A 15% molar PI and 5% molar EHA combination

proves to have one of the largest ranges of success given the time and intensity parameters set forth in the experimental setup for the time and irradiances tested. The resin displays successful one layer cantilever beam prints for 6s to 10s for 13.75mW and 7.5s to 12s for 10mW without deflection post curing. Using this resin formulation, single layer cantilever beam prints and multi-layer 15 degree overhang prints were conducted to prove the feasibility of the system to produce unsupported prints as shown in Figure 6.
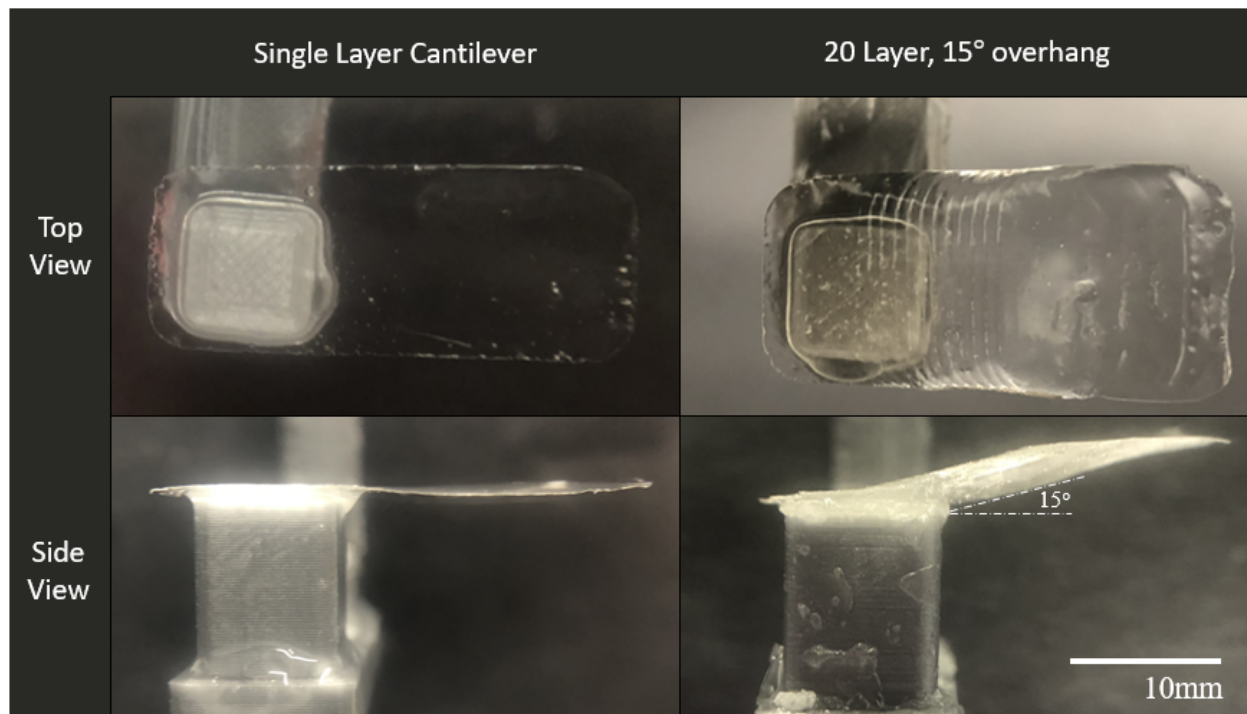

Figure 6: 10% molar PI, 5% molar EHA, 9 seconds of exposure, 10mW intensity trials for a bridge structure and unsupported overhang.

In the left column of Figure 6, printed geometry is displayed 90 degrees from the vertical, with single-layer geometry. The thickness of the single-layer prints was measured to be between 0.20mm and 0.21mm with a homogeneous cure. The unsupported printed geometry of the 15% molar PI resin formulation however, is not necessarily limited to a fluid interface system, as previously expected.

It was hypothesized that the cure depth of the prints were limited by the resin layer thickness between the support fluid and the saline solution. Cure-depth tests for 15% PI resin outside of the system shows that the print depth is constrained near 0.23mm for cures done with and without the supporting solution. In both experiments, an FEP build window was present above the resin. When the same trials were conducted with 10% molar PI, it was observed that the thickness of the cured resin layer was not constrained by the liquid resin layer thickness. This is displayed in figure 7, where cure tests were completed without the supporting solution (denoted in red) to create a working curve [20] for cure depth against experiments where the

support solution was present (denoted in blue). Due to the high PI concentration, cure depths beyond 0.23mm could not be achieved in the cure times tested.
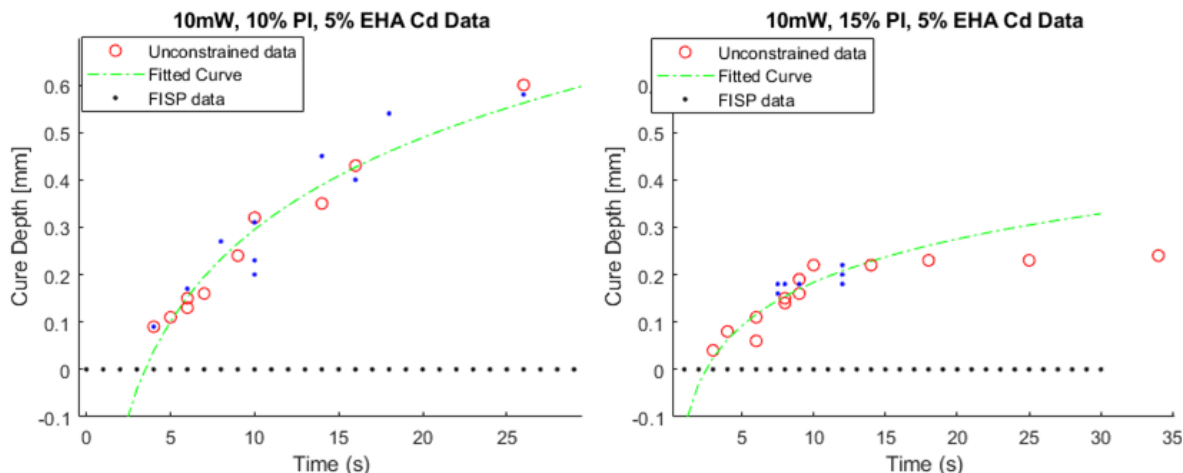

Figure 7: Cure depth curve for 10mW of intensity for two different resin compositions.

To predict the degree of subsequent layers adhering together, absorbance data was taken from a spectrometer for various photoinitiator concentrations as shown in Figure 8.
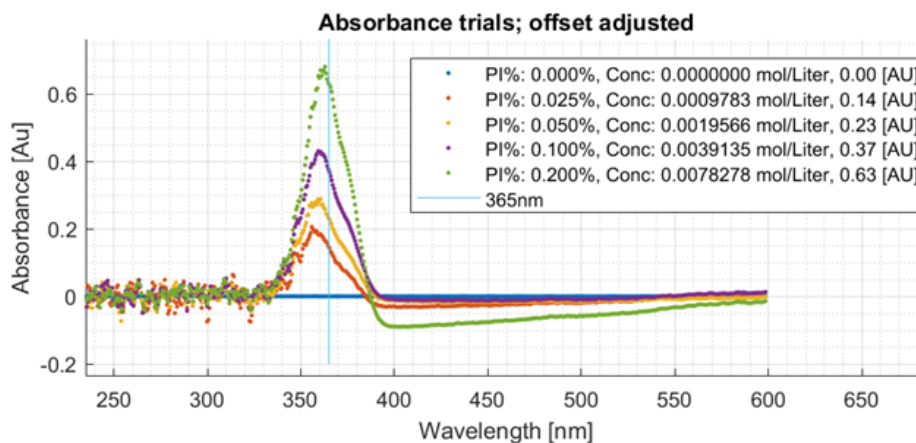

Figure 8: absorptivity data for various photoinitiator concentrations.

Using the Beer-Lambert law [21], the percent of light transmitted for various photoinitiator concentrations can be estimated. From the data, the mean value of the molar absorptivity coefficient, ε, was found to be $104 L\ mol^{-1}\ cm^{-1}$. Using this value for ε, the theoretical transmittance of 365nm spectrum light through a 10% molar PI and 15% molar PI solution for a distance of 0.2mm was found to be 15.0% and 5.7% respectively. Using the fitted critical energy from figure 7 of 490 and 350 $mJ\ *\ cm^{-2}$, the time of irradiance would need to be 23 and 44 seconds for 10% PI and 15% PI respectively to crosslink the resin at a depth of

0.2mm. This result is not reflective of experimental data, as 0.2mm cure depth has been observed at less than ten seconds for both concentrations. This is likely due to the molar concentrations being much higher than the normally accepted concentration of deviation of the Beer-Lambert law of 10mM [22], with concentrations of 0.395 mol/Liter (395mM) and 0.596 mol/Liter (596mM) for the 10% molar PI and 15% molar PI compositions respectively. Cure depth data and experimental observations show that 15% molar PI, 5% molar EHA compositions irradiated at 10mW for nine seconds cure to a depth around 0.20mm, and sufficient layer adhesion occurs when the platform is moved 0.18mm between layers.

Using these parameters, several print tests were performed to evaluate the resin composition inside of the FISP system to generate parts. Bridge geometry with a 2cm overhang was chosen to validate the ability of the system to print unsupported overhangs. The same unsupported part geometry was printed in the FISP system (Top-Down, 15% molar PI, 5% molar EHA, 85% molar HDDA, 10mW Intensity, 9 seconds per layer, 180um layer height) and with a commercial SLA printer (Bottom-up, Formlabs Form 3 printer, black resin, 25um layer height) with results shown in figure 9.

Figure 9: Unsupported bridge geometry comparison between a FISP print and a commercial SLA printer.

The prints from both printing systems highlight some of the advantages and disadvantages of the current FISP setup. When observing the top of the FISP print, voids and rounded corners can be seen due to imperfections in the printing setup. Parts can be weakened from unvacated air during the start of the print and can find its way into the part when raising and lowering subsequent layers, and insufficient resin refill processes sometimes fail to resupply the resin layer. The 8.3 degree beam expansion of the partially-collimated light creates rounded edges that do not follow the exact mask geometry. In the side view, the bridge of the FISP print

is not perfectly level, as both the FEP film and print bed are manually located and subject to placement error. In the FISP print, however, the layers did not delaminate in the unsupported section of the bridge, unlike the commercial SLA print. This can be considered a successful demonstration of the FISP system in reducing support structure necessity. However, the behavior of this particular printed bridge structure is hypothesised to be dependent on the stiff layers formed by the 15% PI resin combination during printing. If the cured layer thickness does not depend on the uncured resin layer thickness in the FISP system, as shown in figure 7, the properties of the 15% molar PI resin formulation could be extrapolated to other printing systems as a method of increasing individual layer stiffness and reducing the relative effects of internal part strains. These characteristics enable the layer to overcome F_{ad}, F_{γ}, and F_{g}, with very low displacement due to internal stresses. Prior literature [15] and experimentation displays an almost complete elimination of the oxygen inhibited dead-zone at 5%wt concentrations of DMPA in HDDA. Successful prints for 15% molar PI displayed significant F_{ad} to overcome, only occurring due to the strength of the individual layer itself. Additionally, more thorough investigation into lower (<2.0% molar PI), more common photoinitiator concentrations needs to occur to truly understand the system's broader merit and feasibility.

Conclusion and Future Work:

Printing layers with sufficient stiffness to overcome internal part stresses from inhomogeneous conversion and prevent delamination has been shown to decrease delamination and dislocation of overhangs in UV-cured parts. The novel system design feasibility of printing a photocurable resin atop a liquid saline solution has been demonstrated with single and multi-layer overhang geometry. Curing experimentation demonstrated internal part stresses as a primary factor in individual layer dislocation and delamination for a large range of photoinitiator concentrations. Further investigation is required to determine if internal stresses from curing can be mitigated in order to thoroughly evaluate whether the buoyancy and gravity balance provided from the FISP system, outlined in figure 2, is sufficient to minimize layer displacement within multi-layer prints. Ongoing investigation is being conducted to quantify and model the force components acting within the system to enhance the system's feasibility justifications. Research is also being conducted into the applicability of various curing techniques, including continuous curing processes in the system.

Acknowledgements

References:

[1] Guo, N., & Leu, M. C. (2013). Additive manufacturing: technology, applications and research needs. Frontiers of Mechanical Engineering, 8(3), 215-243. https://doi.org/10.1007/s11465-013-0248-8

[2] Quan, H., Zhang, T., Xu, H., Luo, S., Nie, J., & Zhu, X. (2020). Photo-curing 3D printing technique and its challenges. Bioactive Materials, 5(1), 110-115. https://doi.org/10.1016/j.bioactmat.2019.12.003

[3] Priedeman Jr, W. R., & Brosch, A. L. (2004). Soluble material and process for three-dimensional modeling.

[4] Yigit, I. E., & Lazoglu, I. Dynamic Build Bed for Additive Manufacturing.

[5] Jiang, J., Xu, X., & Stringer, J. (2018). Support Structures for Additive Manufacturing: A Review. Journal of Manufacturing and Materials Processing, 2(4). https://doi.org/10.3390/jmmp2040064

[6] Zhang, N., Zhang, L.-C., Chen, Y., & Shi, Y.-S. (2019). Local Barycenter Based Efficient Tree-Support Generation for 3D Printing. Computer-Aided Design, 115, 277-292. https://doi.org/https://doi.org/10.1016/j.cad.2019.06.004

[7] Wei, X., Qiu, S., Zhu, L., Feng, R., Tian, Y., Xi, J., & Zheng, Y. (2018). Toward Support-Free 3D Printing: A Skeletal Approach for Partitioning Models. IEEE Transactions on Visualization and Computer Graphics, 24(10), 2799-2812. https://doi.org/10.1109/TVCG.2017.2767047

[8] Lee, M. P., Cooper, G. J. T., Hinkley, T., Gibson, G. M., Padgett, M. J., & Cronin, L. (2015). Development of a 3D printer using scanning projection stereolithography. Scientific Reports, 5(1), 9875. https://doi.org/10.1038/srep09875

[9] Bhanvadia, A. A., Farley, R. T., Noh, Y., & Nishida, T. (2021). High-resolution stereolithography using a static liquid constrained interface. Communications Materials, 2(1), 41. https://doi.org/10.1038/s43246-021-00145-y

[10] Nishida, T., & Bhanvadia, A. A. (2020). Three-dimensional fabrication at inert immiscible liquid interface. In: Google Patents.

[11] Robeson, L. M., Samulski, E. T., Ermoshkin, A., & DeSimone, J. M. (2019). Continuous three dimensional fabrication from immiscible liquids.

[12] Koros, W. J., Wang, J., & Felder, R. M. (1981). Oxygen permeation through FEP Teflon and Kapton polyimide. Journal of Applied Polymer Science, 26(8), 2805-2809. https://doi.org/10.1002/app.1981.070260832

[13] Bhushan, B. (2003). Adhesion and stiction: Mechanisms, measurement techniques, and methods for reduction. Journal of Vacuum Science & Technology B: Microelectronics and Nanometer Structures Processing, Measurement, and Phenomena, 21(6), 2262-2296. https://doi.org/10.1116/1.1627336

[14] The Complete Sodium Chloride Density-Concentration Table Calculator. (n.d.). https://www.handymath.com/cgi-bin/nacltble.cgi?submit=Entry.

[15] Hoyle, C. E. (2004). An overview of oxygen inhibition in photocuring. Technical Conference Proceedings-UV & EB Technology Expo & Conference, Charlotte, NC, United States,

[16] Tumbleston, J. R., Shirvanyants, D., Ermoshkin, N., Janusziewicz, R., Johnson, A. R., Kelly, D., Chen, K., Pinschmidt, R., Rolland, J. P., Ermoshkin, A., Samulski, E. T., & DeSimone, J. M. (2015). Continuous liquid interface production of 3D objects. Science, 347(6228), 1349-1352. https://doi.org/10.1126/science.aaa2397

[17] Karalekas, D., & Aggelopoulos, A. (2003). Study of shrinkage strains in a stereolithography cured acrylic photopolymer resin. Journal of Materials Processing Technology, 136(1), 146-150. https://doi.org/https://doi.org/10.1016/S0924-0136(03)00028-1

[18] Chartoff, R., & Du, J.-Z. (1995). Photopolymerization Reaction Rates By Reflectance Real Time Infrared Spectroscopy: Application To Stereolithography Resins.

[19] Decker, C. (1996). Photoinitiated crosslinking polymerisation. Progress in Polymer Science, 21(4), 593-650. https://doi.org/https://doi.org/10.1016/0079-6700(95)00027-5

[20] Jacobs, P. F. (1992). Fundamentals of stereolithography. 1992 International Solid Freeform Fabrication Symposium,

[21] Born, M., Wolf, E., & Bhatia, A. B. (2019). *Principles of optics*. Cambridge University Press.

[22] Mehta, A. (2016, June 27). *Ultraviolet-Visible (UV-Vis) Spectroscopy – Limitations and Deviations of Beer-Lambert Law*. PharmaXChange.Info.https://pharmaxchange.info/2012/05/ultraviolet-visible-uv-vis-spectroscopy-%e2%80%93-limitations-and-deviations-of-beer-lambert-law/

Appendix

Name	Acronym	Viscosity (cP)	Density (g/mL)	Water solubility (mg/mL)	Active/Inert
2-Ethylhexyl acrylate	EHA	1.7	0.885	0.10	Active
1,6-Hexanediol diacrylate	HDDA	9	1.02	0.10	Active
Decahydronaphthalene	Decalin	1.788	0.896	0.10	Inert
Xylenes	-	0.812	0.865	0.10	Inert
Butyl Acrylate	BA	0.92	0.9	0.14	Active
n-Butyl Acetate	-	1.1002	0.8825	0.68	Inert
Triethylene glycol dimethacrylate	TEGDMA	50	1.072	2.41	Active
Urethane dimethacrylate	UDMA	6.75	1.129	6.62	Active
Methyl Methacrylate	MMA	0.6	0.94	15.00	Active
Propylene glycol methyl ether acetate	PGMEA	0.8	0.962	19.80	Active
Methyl Acrylate	MA	0.6	0.95	50.00	Active
1,3-Propanediol	-	52	1.0597	Miscible	Active
BYK UV-3500	Silicon	Unk.	1.04	Unk.	Active

Figure A1: Various additives compared for water solubility, density, and viscosity.